

# Lawrence Berkeley National Laboratory

## Lawrence Berkeley National Laboratory

### **Title**

Real-time high-resolution X-ray imaging and nuclear magnetic resonance study of the hydration of pure and Na-doped C3A in the presence of sulfates

### **Permalink**

<https://escholarship.org/uc/item/2df633g9>

### **Author**

Kirchheim,, A. P.

### **Publication Date**

2011-01-19

### **DOI**

10.1021/ic101460z

## Real-time high-resolution X-ray imaging of the hydration of pure and Na-doped C<sub>3</sub>A in different suspensions

A. P. Kirchheim<sup>a,c,\*</sup>, D.C. Dal Molin<sup>a</sup>, P. Fischer<sup>b</sup>, Abdul-Hamid Emwas<sup>c</sup>,

J. L. Provis<sup>d</sup> and P.J.M. Monteiro<sup>e</sup>

<sup>a</sup> *Department of Civil Engineering*

*Federal University of Rio Grande do Sul, Porto Alegre, RS, Brazil*

<sup>b</sup> *Center for X-ray Optics, Lawrence Berkeley National Laboratory, Berkeley CA USA*

<sup>c</sup> *NMR Core lab, King Abdullah University of Science and Technology, Thuwal 23955-6900, Kingdom of Saudi Arabia,*

<sup>d</sup> *Department of Chemical & Biomolecular Engineering, University of Melbourne, Victoria 3010, Australia*

<sup>e</sup> *Department of Civil and Environmental Engineering  
University of California, Berkeley, CA, USA*

### ABSTRACT

This study details the differences in real-time hydration between pure (cubic) and Na-doped (orthorhombic) C<sub>3</sub>A. First, pure phases were synthesized in the laboratory to develop an independent benchmark for the reactions, then the reactions of others phases were isolated. Because the kinetics of this reaction moves extremely quickly, most methods are not adequate to study the reactions in the early phases. Here, a high-resolution full-field soft X-ray imaging technique operating in the X-ray water window was used to capture the mechanism of the C<sub>3</sub>A hydration. The results show that there are differences in the hydration mechanism of each type of C<sub>3</sub>A, dependent on the concentration of sulfates ions in solution. The reactions with cubic C<sub>3</sub>A (pure) seems to be more susceptible to higher concentrations of sulfate ions by forming smaller ettringite needles at a slower pace than the orthorhombic C<sub>3</sub>A (Na-doped) sample.

**Keywords:** tricalcium aluminate, hydration, hydration products, ettringite, image analysis

### 1. Introduction

The properties of clinkers are strongly affected by the quantity and composition of the clinker phases [1], which can drive the kinetic process of hydration. The hydration of C<sub>3</sub>A is an important stage in the overall hydration of cement because it has considerable influence on its setting and early hardening. The hydration of C<sub>3</sub>A is far more strongly affected by environment conditions than that of C<sub>3</sub>S and, in particular, by the presence of other substances with which it can react [8]. The reaction of C<sub>3</sub>A with water is a primary consideration. Calcium aluminate hydrates (e.g., C<sub>3</sub>AH<sub>6</sub>, C<sub>4</sub>AH<sub>19</sub>, and C<sub>2</sub>AH<sub>8</sub>) form quickly and liberate large amounts of heat [9]. If the very rapid and exothermic hydration of C<sub>3</sub>A is allowed to proceed unhindered in cement, then the setting occurs too quickly and the cement paste does not develop strength. Therefore, calcium sulfate is added to slow down the C<sub>3</sub>A hydration. In the presence of gypsum, C<sub>3</sub>A forms needle-like ettringite. Thus, for practical purposes, it is not the hydration reaction of C<sub>3</sub>A alone that is important but the hydration reaction of C<sub>3</sub>A in presence of gypsum (sulfates). The reactivity of C<sub>3</sub>A in clinker and the availability of sulfate in solution control the setting characteristics of concrete, making these compounds ideal for addressing probable setting problems.

Because of the high contents of C<sub>3</sub>A in some cement, special attention must be paid to the mineralogy and reactivity of this phase. Industrial clinkers and their phases contain minor elements such as Na<sub>2</sub>O, K<sub>2</sub>O, SO<sub>3</sub>, and Cl<sup>-</sup>, which may be attributed to several sources, such as raw materials, fuel and/or the lining of the kilns. Alkalis can be incorporated into a number of phases of the clinker and often Na<sub>2</sub>O is

---

\* Corresponding author: Tel.: +55 51 3308 3518; Fax: +55 51 3308 3321. *E-mail address:* anapaula.k@gmail.com

taken up by the  $C_3A$  [2]. When  $C_3A$  is synthesized in the presence of alkalis, its crystal lattice changes and the formation of the other phases occur [3]. There are several series of solid solutions with the general formula  $Na_{2x}Ca_{3-x}Al_2O_6$ , including a cubic  $C_3A$  with  $0 < x < 0.10$ , an orthorhombic  $C_3A$  with  $0.16 < x < 0.20$ , and a monoclinic  $C_3A$  with  $0.20 < x < 0.25$  [4]. The most important solid solutions series occurring in this system ( $Na_{2x}Ca_{3-x}Al_2O_6$ ) are the orthorhombic and monoclinic [5].

In Portland cements, the cubic or orthorhombic  $C_3A$  are found alone or in combination; the monoclinic modification has not been observed. The cubic phase is often finely grained and closely mixed with dendritic crystals of ferrite. The orthorhombic modification occurs as a prismatic, dark interstitial material, and it is sometimes pseudo tetragonal [4]. In the orthorhombic structure, the replacement of  $Na^+$  at a calcium site can only occur at the  $Ca_5$  site, which causes the polyhedron to expand [6]. In industrial clinkers, a more typical mechanism of formation of this phase is the metastable extension of the solid solution series accompanied by rapid cooling [5]. In cement, higher percentages of  $Na_2O$  in the raw materials lead to formation of orthorhombic  $C_3A$  [7].

This paper aims to clarify the early hydration of cubic and orthorhombic  $C_3A$  using advanced *in-situ* technique by means of soft X-ray microscopy, which allows studying hydration in a wet environment with nanometer spatial resolution. The present study uses pure components of cubic  $C_3A$  (pure) and orthorhombic  $C_3A$  (Na-doped) synthesized in a laboratory. This allows for isolating and observing the effects of each crystalline form of the aluminate in a given solution, which would not be possible if cement particles (containing several different phases) were used. In addition, different concentrations of sulfate ions were analyzed to understand how each aluminate works in different conditions. This study is part of a larger work [10] that includes the study of these materials in other conditions and using other techniques. Also some previous results were published by Kirchheim et al [11].

## 2. Experimental Section

### 2.1 Materials

Samples of tricalcium aluminate ( $C_3A$ )—orthorhombic (Na-doped) and cubic (pure)—were obtained from Construction Technology Laboratories, Inc., Skokie, IL. Both compounds were synthesized in a laboratory by heating a stoichiometric blend of reagent grade  $CaCO_3$  and alumina ( $Al_2O_3$ ) in an electric furnace at  $1400\text{ }^\circ\text{C}$  for 1 hour, followed by quenching in air. The orthorhombic  $C_3A$  was prepared from reagent grade  $CaCO_3$ ,  $Al_2O_3$ , and  $Na_2CO_3$  in stoichiometric proportion similar to that reported by Regourd et al [12], with the latter slightly added in excess to account for alkali volatilization during the synthesizing process. After synthesizing, each material was processed in a ceramic mill to 325 mesh.

XRD, using a PANalytical XPert Pro and thermal analysis (TA) TA Instruments, model SDT 2960, were done to confirm phase composition, purity and conditions of the sample. Comparison of the peak positions were made with data from Regourd et al [12] (ICDD PDF No.38-1429 for the cubic sample and ICDD PDF No.26-0958 for the orthorhombic one). The TA analysis showed that the sample were keep no hydrated by the air moisture because it presented a low loss of mass – less then 1% and 8%, respectively for cubic and orthorhombic sample.

Particle size distributions of the samples were done in a CILAS 1180 Laser Granulometer, in isopropyl alcohol of 99,5% of purity based liquid media; the results are presented in Table 1. The lower size of this equipment was 40nm and was applied the Fraunhofer Approximation.

Table 1: particle size distribution of the sample by means of laser granulometry

|               | Cubic $C_3A$ ( $\mu\text{m}$ ) | Orthorhombic $C_3A$ ( $\mu\text{m}$ ) |
|---------------|--------------------------------|---------------------------------------|
| 10% diameter  | 5,74                           | 1,64                                  |
| 50% diameter  | 24,31                          | 16,04                                 |
| 90% diameter  | 45,00                          | 36,34                                 |
| mean diameter | 25,16                          | 18,43                                 |

### 2.2 Sample preparation

### 2.2.1 Imaging with Soft X-Ray Microscopy

Soft X-ray microscopy operating in the water window, i.e. at a photon wavelength of about 2.4nm, combines high spatial resolution in the tens of *nm* range with the ability to penetrate several  $\mu\text{m}$  of aqueous solution, making it an ideal *in-situ* technique to study wet and nano-structured materials. The high spatial resolution of this microscopy technique is well suited for observing the formation of ettringite crystals around the calcium aluminate grains and in solution, and to see the differences between the hydrates formed from cubic and orthorhombic  $\text{C}_3\text{A}$ . Furthermore, because the sample is kept wet at all times, it is possible to observe the progression of hydration over time.

Real-time hydration studies with soft X-Ray transmission microscopy was done at the full field soft X-ray microscopy end-station XM-1 located at the beam line 6.1.2 at the Advanced Light Source (ALS) in Berkeley CA. The microscope is jointly operated by the Center for X-ray Optics and the ALS and the X-ray optical setup of XM-1 is described elsewhere [13]. Recent achievements in using Fresnel zone plates (FZP) for X-ray optics allow for a spatial resolution down to 15nm [14, 15]. Synchrotron radiation emitted from a bending magnet is passed through the first FZP, a condenser zone plate, which provides both a partially coherent hollow-cone illumination of the specimen, and, in combination with a pinhole, serves as linear monochromator to select the proper wavelength. After transmitting the sample, a micro zone plate (MZP) projects a full-field image onto an X-ray sensitive CCD camera. For this study, a 35nm MZP was used and imaged at a magnification of about 2000. The illumination time per image was between 1-14 seconds. Each image covers a field of view of about  $10\mu\text{m}$ .

The liquid media, composed of a saturated solution with calcium hydroxide (CH) and calcium sulfate dehydrate (gypsum,  $\text{C}\bar{\text{S}}\text{H}_2$ ), was selected to provide sulfate ions to stimulate both the formation of ettringite and the chemical composition of the pore solution in fresh cement pastes. After mixing gypsum and calcium hydroxide for 24 hours the solution was filtered twice. To avoid carbonation, the solution was prepared and stored in a glove bag filled with nitrogen gas. Also to avoid the possibility of an alkali-silica reaction, polyethylene and Teflon beakers, flasks, and pipettes were used. Dispersions of both  $\text{C}_3\text{A}$  forms were prepared with the saturated solution, which presented a solution/aluminate ratio of 5 ml/g, 10 ml/g, and 50 ml/g. The amounts of reagents used to prepare the dispersions were 0.4g, 0.2g and 0.04g of  $\text{C}_3\text{A}$  and 2 ml of the saturated solution, respectively. The solid particles were hand-mixed for 50 seconds in the solution and then centrifuged for 15 seconds. Therefore, in this study the solution/aluminate ratio is called the initial solution/aluminate ratio ( $s/a_{\text{initial}}$ ). During this first minute of hydration, it is expected that aluminum and calcium-bearing ions are released into the solution from the dissolution of the  $\text{C}_3\text{A}$  particles. The number of nuclei formed during the initial period will be affected by the solution/aluminate ratio; the number of nuclei formed initially may then play an important role in determining the growth rates of ettringite or other hydrates after dilution. To allow for sufficient transmission of the soft X-rays, a small droplet—containing small solid particles—was taken from the supernatant solution and assembled in a specialized sample holder, comprising of two silicon nitride windows, where the solution is squeezed in between to an appropriate thickness and then imaged. This procedure is described in detail in Silva and Monteiro [16] and Monteiro et al [17].

## 3. Results and discussion

The hydrated products were observed to form within a few minutes after mixing the cubic and three different initial solution/aluminates. Results are presented below.

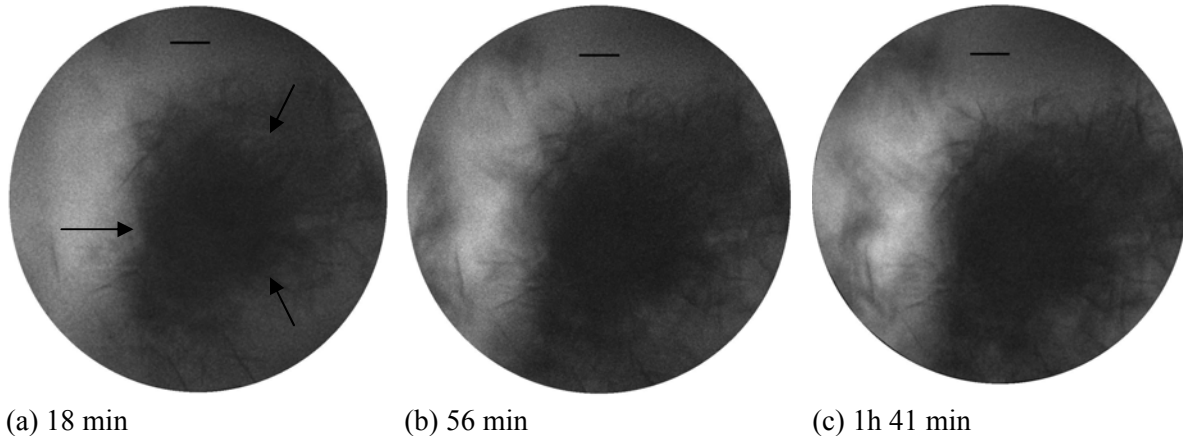
### 3.1 Initial solution/aluminate ratio = 5 ml/g

- **Cubic  $\text{C}_3\text{A}$**

Figure 1 shows images of the cubic  $\text{C}_3\text{A}$  hydration in a saturated solution of calcium hydroxide and gypsum; the image of the sample was taken in the same specimens at two different positions. The images from Position 1, recorded from 18 minutes to 1 hour and 41 minutes, show the cubic  $\text{C}_3\text{A}$  particle

(indicated by arrows) covered by hydration products. The images of hydration evolution in Position 2, recorded from 50 minutes to 1 hour and 28 minutes, show an ettringite agglomeration. In a few minutes all particles completely hydrate inside their original boundaries. Other 3 specimens were analyzed and also presented the same morphology.

### Position 1

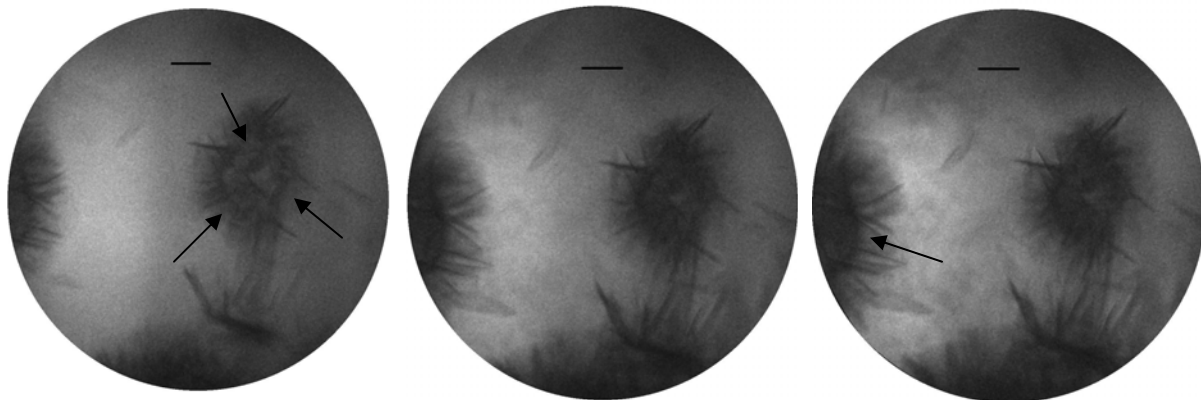


(a) 18 min

(b) 56 min

(c) 1h 41 min

### Position 2



(a) 50 min

(b) 1 h 8 min

(c) 1h 28 min

Figure 1 – *in-situ* soft x-ray images of hydrating cubic  $C_3A$  particles in a saturated calcium hydroxide-gypsum solution,  $s/a_{\text{initial}} = 5$  ml/g. Hydration time is indicated. Sample 1 and 2. Scale bar corresponds to  $1 \mu\text{m}$

In all images, the products of hydration are fibrous-like. The morphology identified suggests that crystals are acicular ettringite, which precipitated instantly. Silva and Monteiro [16], however, observed that cubic  $C_3A$  particles in the same type of solution resulted in  $C_3A$  particles being covered by a continuous or discontinuous hydrated layer. X-ray diffraction and thermal analyses pointed by the authors revealed that the sample still contained 31% of  $\text{Ca}(\text{OH})_2$ , which was originally used as a raw material for synthesizing the  $C_3A$ .

- **Orthorhombic  $C_3A$**

Figure 2, shows large long fibers-like crystals [needles and hexagonal platelets that can be seen in a plan view (note the appearance of transparent hexagons) or a lateral view (note the long needles)], with a length of 3 to 5  $\mu\text{m}$ , in a solution with several orthorhombic  $C_3A$  particles. The particles seem to be surrounded by a gel (indicated by the arrows). These particles in the form of needles and platelets

disappear over time; after 49 minutes are no longer present in the sample. Note that the orthorhombic  $C_3A$  particles suffered substantial swelling during hydration (indicated by the circumference and the arrows). It is also observed an agglomeration/approximation of the particles over time.

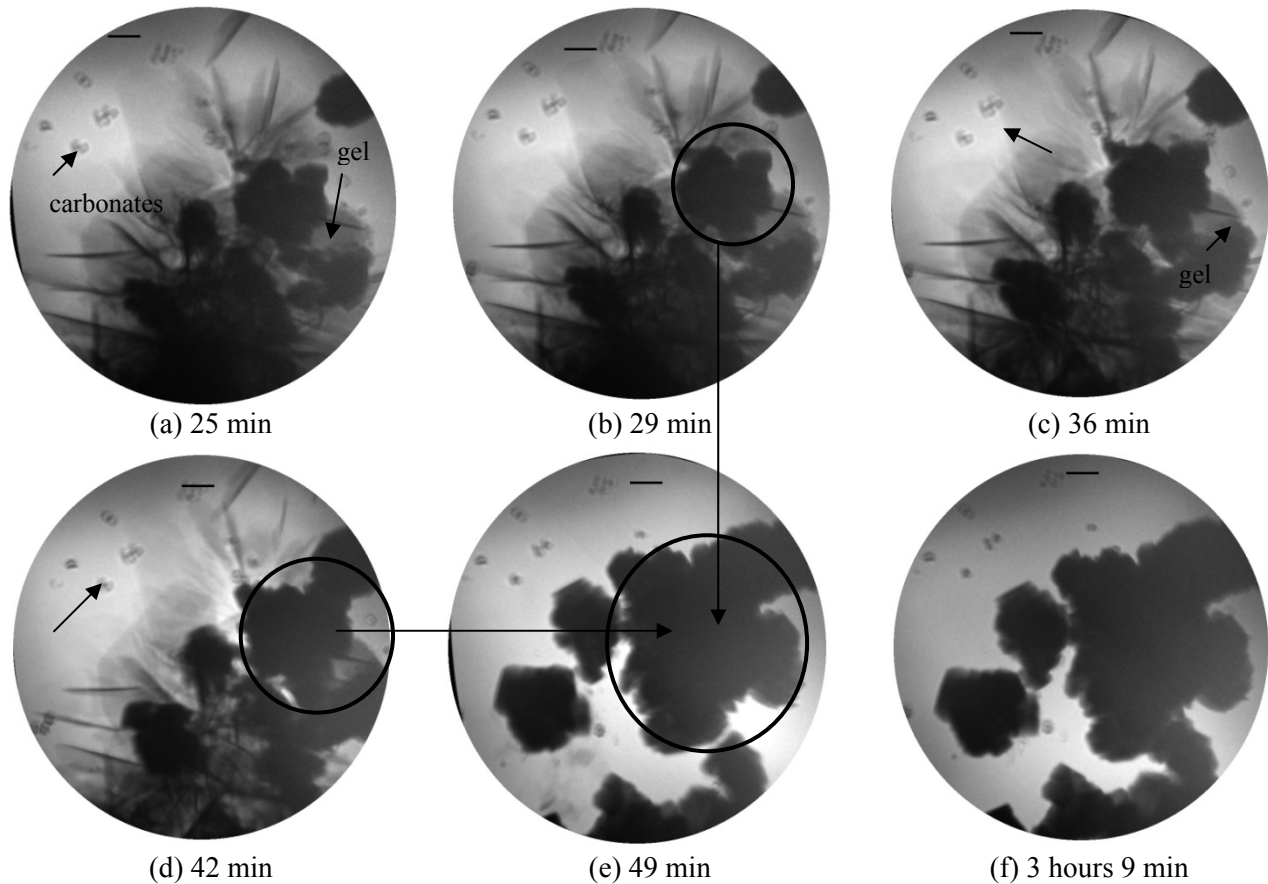


Figure 2 – *in-situ* soft x-ray images of hydrating orthorhombic  $C_3A$  particles in a saturated calcium hydroxide-gypsum solution,  $s/a_{\text{initial}} = 5$  ml/g. Hydration time is indicated. Sample 1. Scale bar corresponds to 1  $\mu\text{m}$

In the orthorhombic specimen, the reactions evolved as expected until at 50 minutes of hydration; no modifications were observed after this period. Although the aspect of the orthorhombic  $C_3A$  hydration in the same suspension ( $s/a_{\text{initial}} = 5$  ml/g) is completely different than the cubic  $C_3A$  hydration previously shown, it does not necessarily mean that the cubic is more reactive, however, it does mean it works in a different way, principally by means of the morphology of the particles and products formed. This differences can be explained based in Glasser and Marinho [20] ideas, which proposed that the hydration of Na-doped  $C_3A$  (orthorhombic  $C_3A$ ) can be summarized as the broken off the Na-O bonds which lead to the formation of mobile  $\text{Na}^+$  ions where  $\text{Ca}^{2+}$  is only partially hydrolyzed in this zone. In the vicinity or the alumina-rich zone, more general hydrolysis occur and oxide ions, formerly linked to  $\text{Ca}^{2+}$  an  $\text{Al}^{3+}$ , convert to OH- groups, which together with appropriate cations are available to participate in the reconstituted surface film. Ions steadily flow into the solution, whose ionic strength and basicity increases at least up to the point at which precipitations begins.

*b) Initial solution/aluminate ratio = 10 ml/g*

In order to evaluate the effect of higher sulfate ions concentrations in solution and to facilitate the observation of the cubic  $C_3A$  particles hydrating, the initial solution/aluminate ratio was increased to 10 ml/g.

- **Cubic  $C_3A$**

In a higher solution/aluminate ratio, unlike the images showed previously (figure 1), these allow us to observe the particles being hydrated over time more clearly and slower.

From the beginning of the analysis (Figure 4), the particles are immediately covered by needle-like hydrates that grow in length and thickness over time (mainly between 53 minutes and 1 hour and 19 minutes). Changes in the ionic concentration over time might explain the instability of the ettringite and formation of large crystals [16].

**Position 1**

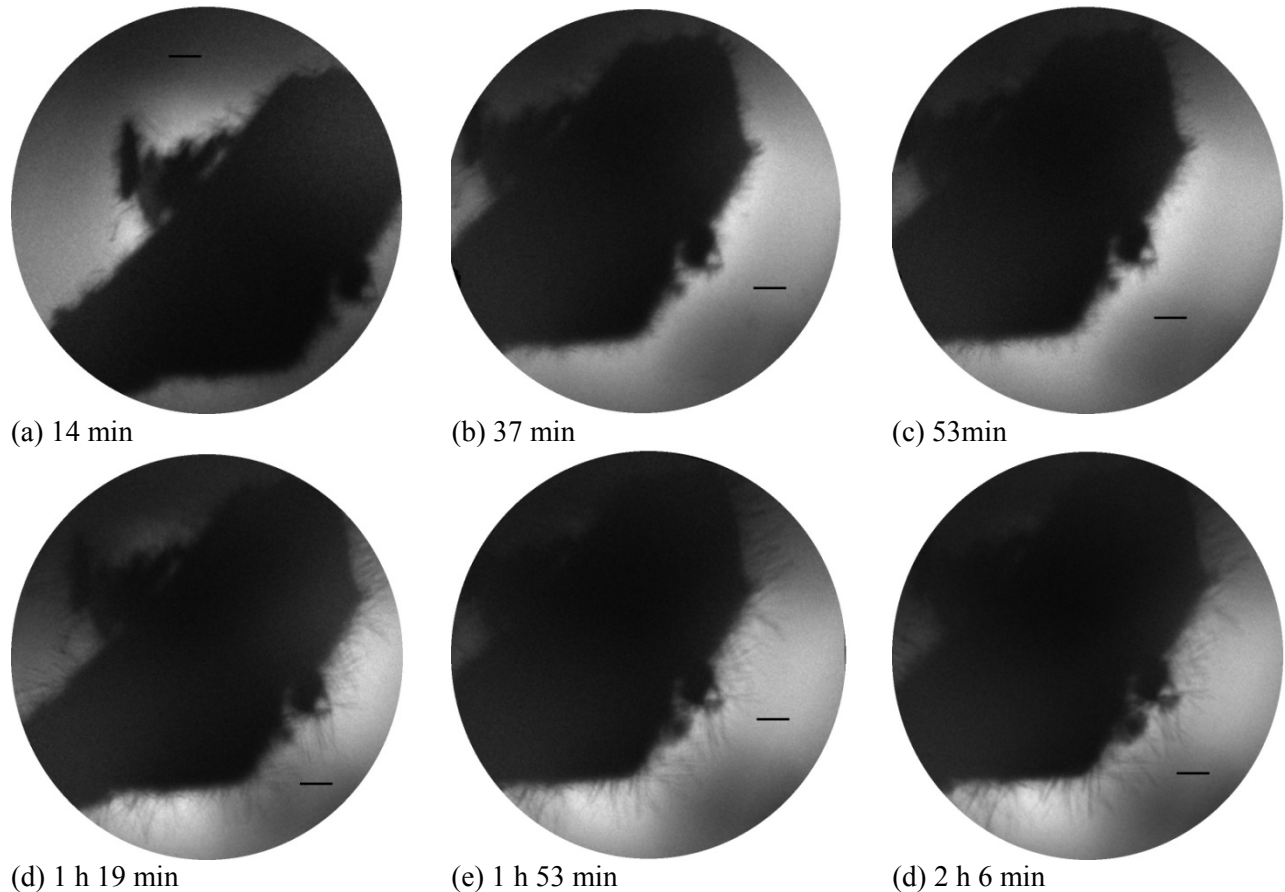


Figure 4 – *in-situ* soft x-ray images of hydrating cubic  $C_3A$  particles in a saturated calcium hydroxide-gypsum solution,  $s/a_{\text{initial}} = 5$  ml/g. Hydration time is indicated.

Sample 1. Scale bar corresponds to 1  $\mu\text{m}$

- **Orthorhombic  $C_3A$**

Figure 5 presents two positions in the same sample of orthorhombic  $C_3A$  particles hydrating in a saturated calcium hydroxide-gypsum solution. Position 1 shows images from 40 min to up 2 hours. Compared to cubic  $C_3A$  hydration, the orthorhombic  $C_3A$  seemed to **increase the aspect ratio of** ettringite crystals. The same gel that appeared in Figure 3 can be seen again, a possible precursor of ettringite formation (See Figure 5 at Position 2). Some researchers [4, 24] believe that there is a change in the morphology of the ettringite at the end of the induction period. This is initially deposited as a gel-like material and, according

to this view, changes into a crystalline needle-like form. Unlike the crystalline form, ettringite gel is impermeable to water. In a mixture with cement and water, Billingham and Coveney [24] posed that an initial jump in the slurry consistency at early stages is due to the rapid formation of ettringite gel on mixing.

#### Position 1

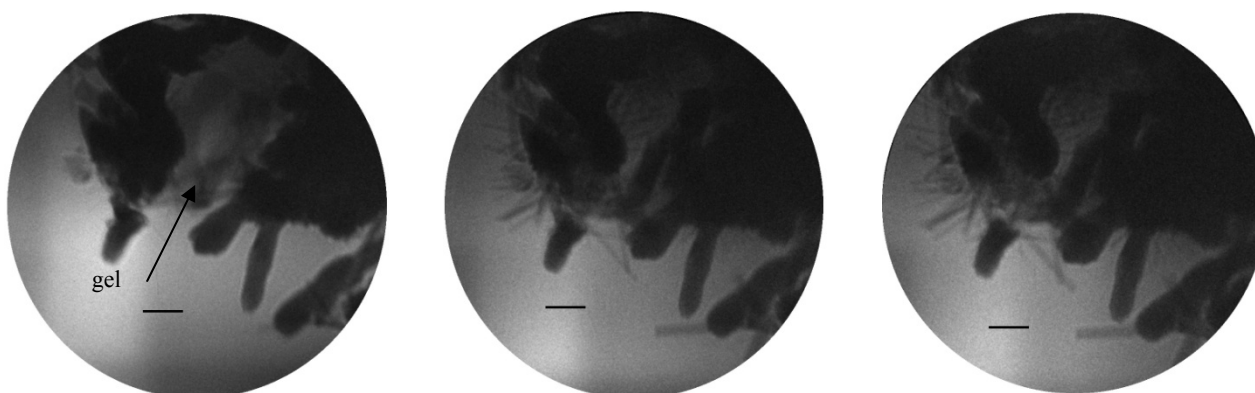


(a) 40 min

(b) 1 h 27 min

(c) 2 h 28 min

#### Position 2



(a) 19 min

(b) 43 min

(c) 2 hours

Figure 5 – *in-situ* soft x-ray images of hydrating orthorhombic  $C_3A$  particles in a saturated calcium hydroxide-gypsum solution,  $s/a_{\text{initial}}=10$  ml/g. Hydration time is indicated. Sample 1, Positions 1, 2. Scale bar corresponds to 1  $\mu\text{m}$

Both forms of  $C_3A$  in this suspension ( $s/a_{\text{initial}}=10$  ml/g) presented differences in morphology when compared to the previous suspension ( $s/a_{\text{initial}}=5$  ml/g); this can be attributed to the increased concentration of sulfates, which allow the ettringite formation close to the  $C_3A$  particles. In summary: (a) the hydration of cubic  $C_3A$  hydration shows ettringite needles forming along the surface of the particle, which are smaller than those observed in orthorhombic  $C_3A$ ; and (b) in orthorhombic  $C_3A$  hydration an intermediate gel stage occurred before the formation of long ettringite needles.

c) *Initial solution/aluminate ratio = 50 ml/g*

To complement the analysis of the effect of sulfate ions concentration and verify further the influence of the initial solution/aluminate ratio in the hydration reaction of cubic and orthorhombic  $C_3A$ , it was increased to  $s/a_{\text{initial}}=50$  ml/g.



- **Cubic C<sub>3</sub>A**

The aspect of the cubic C<sub>3</sub>A particles hydrating in a higher initial solution/aluminate ratio is presented in Figure 6. Note how different this image is compared to the previous images. Here, it is possible to observe the needles growing and sometimes a complete dissolution of the C<sub>3</sub>A particles occurred, with precipitation of needle-like crystals of ettringite.

**Position 1**

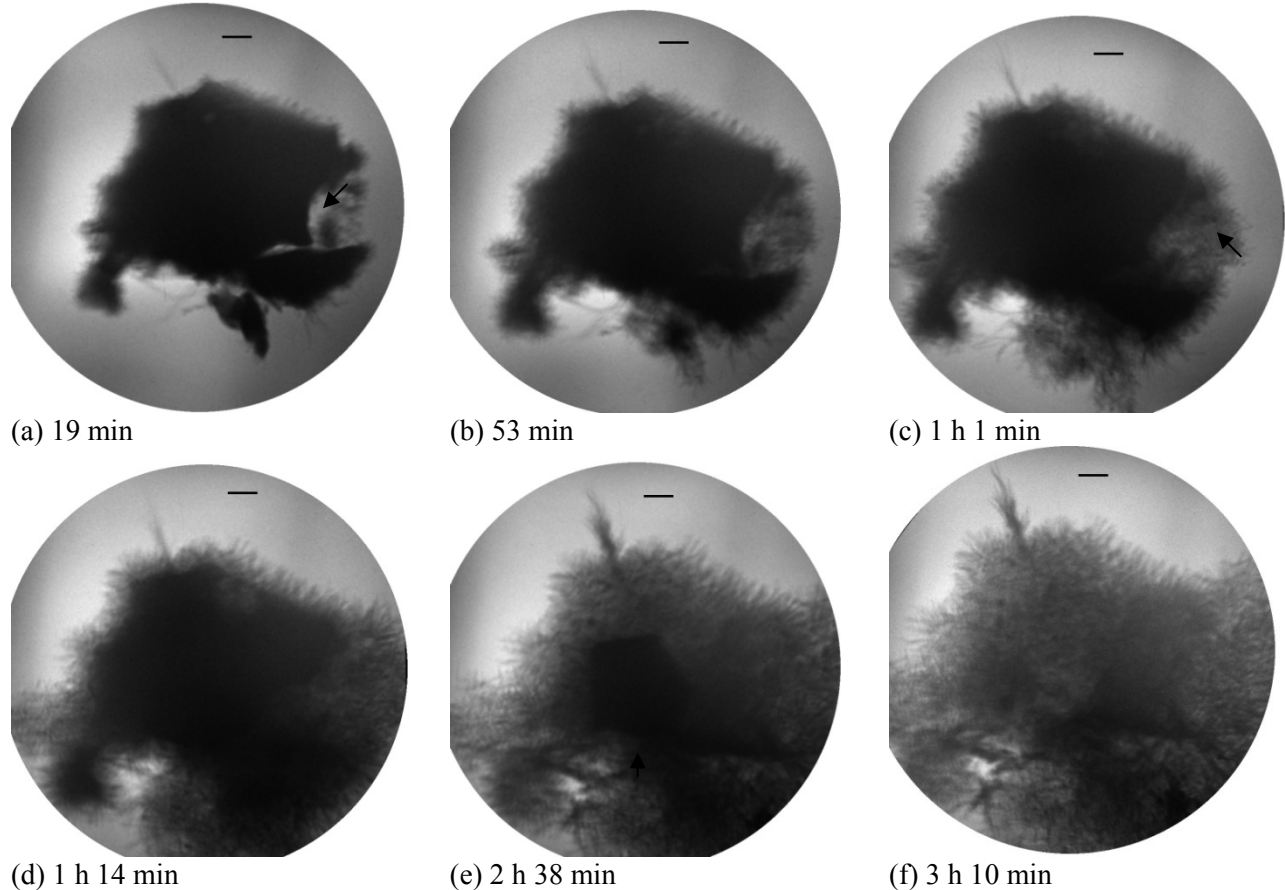


Figure 6 – *in-situ* soft x-ray images of hydrating cubic C<sub>3</sub>A particles in a saturated calcium hydroxide-gypsum solution,  $s/a_{\text{initial}} = 50$  ml/g. Hydration time is indicated. Sample 1, Position 1. Scale bar corresponds to 1  $\mu\text{m}$

Position 1 (Figure 6) shows the hydration of the particles starting at 11 minutes, which is first covered by hydrates and then followed by a rapid length and thickness growth up to the first 50 minutes after mixing. After this period, the C<sub>3</sub>A particle (which is completely covered by numerous needles-like hydrates) starts to be transformed in ettringite. From these images, the trough-solution mechanism of ettringite formation can be seen; basically there is interface dislocation of outer products to inner products. The cubic C<sub>3</sub>A particle—initially with a dense structure—at the end of 3 hours is fully transformed into a structure of ettringite needles. The C<sub>3</sub>A particle is completely consumed. The original boundary of the C<sub>3</sub>A particle increases and the observation space is mainly occupied by ettringite needles.

- **Orthorhombic C<sub>3</sub>A**

Figure 8 present orthorhombic C<sub>3</sub>A particles hydrating at 54 minutes to 4 hours in a saturated calcium hydroxide-gypsum solution. Note that the orthorhombic samples exhibits almost identical behavior to that observed for the cubic sample in Figure 7. If the same particle

size is considered, a layer of small needles is readily visible growing in the surface of the particle and some swelling of the particle [as indicate the arrows in image (a) and (c)]. One key difference between the cubic sample and the orthorhombic sample is the appearance of several long needles that form close and around the particle and in solution. Needles can also be observed far away from the particle. Comparing Figs 9 a-c, suggests that some initial products formed away from the surface of the C<sub>3</sub>A are lost - rather than formed - over time. The growth of acicular hydrates occurs with greater intensity after 1 hour; the reactions apparently stabilized after 2 hours.

#### Position 1

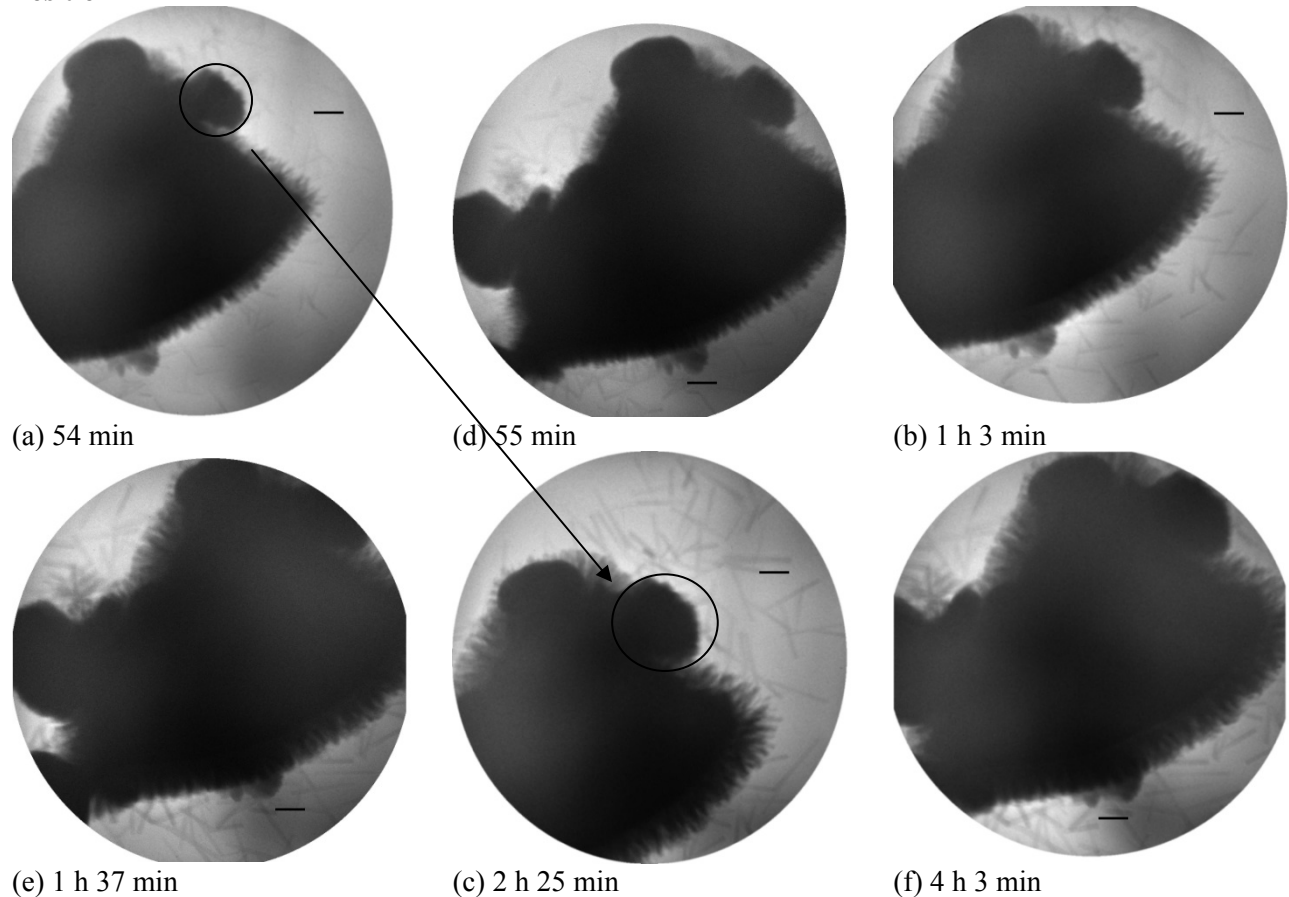


Figure 8 – *in-situ* soft x-ray images of hydrating orthorhombic C<sub>3</sub>A particles in a saturated calcium hydroxide-gypsum solution,  $s/a_{\text{inicial}} = 50$  ml/g. Hydration time is indicated. Sample 1, Position 1. Scale bar corresponds to 1  $\mu\text{m}$

The through-solution mechanism (dissolution/precipitation) of ettringite formation can be seen in Figure 9. A comparison between the orthorhombic particles shown in Figure 9 with the cubic particles shown in Figure 6 shows that the orthorhombic C<sub>3</sub>A form larger and thicker needles-like crystals over time. Observing Figure 8 and 9 we can notice the variation in behavior between smaller and larger grains.

#### Position 2

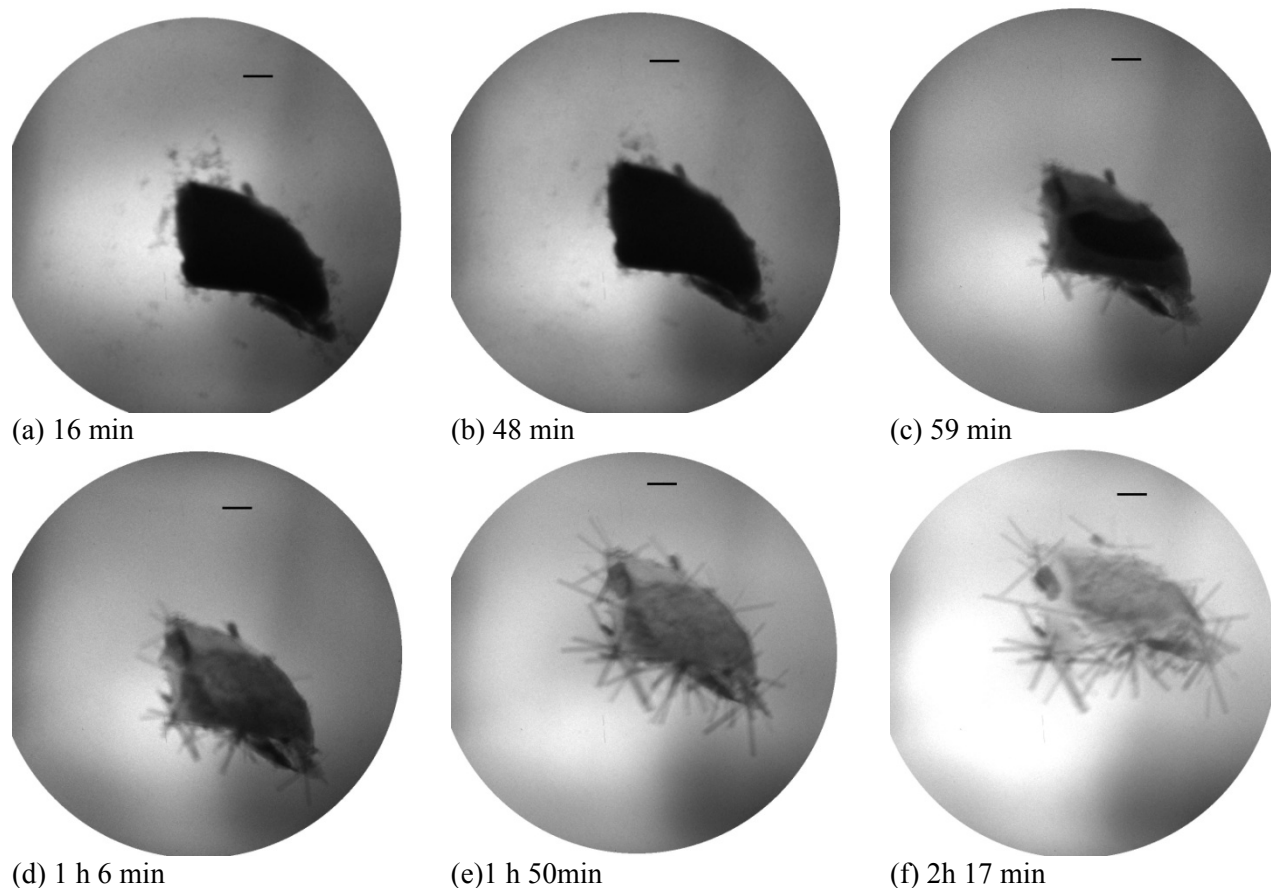


Figure 9 – *in-situ* soft x-ray images of hydrating orthorhombic  $C_3A$  particles in a saturated calcium hydroxide-gypsum solution,  $s/a_{\text{inicial}} = 50$  ml/g. Hydration time is indicated. Sample 1, Position 2. Scale bar corresponds to 1  $\mu\text{m}$

Contrary to the results obtained in the previous specimens ( $s/a_{\text{inicial}} = 5$  and  $10$  ml/g), in this suspension ( $s/a_{\text{inicial}} = 50$  ml/g) the through-solution mechanism of ettringite formation can be observed for both specimens (cubic and orthorhombic), varying quite strongly when the initial solution/aluminate ratio is increased. In summary, the through-solution rates can be distinguished from ion exchange and absorption.

Finally, it is interesting to note that in all positions of both the cubic and orthorhombic samples for these conditions, the reactions happen mostly after 50 minutes of hydration. This is explained by the higher interparticle distance and the higher sulfate ions concentration. In a cement matrix a high water cement ratio has been shown to lead to better diffusion of the ions in the pore solution leading to the formation of more ettringite crystals, especially away from the surface of cement particles [9].

Any crystallization process comprise three basic steps: achievement of supersaturation; formation of crystal nuclei, and growth of particles [25]. The difference in chemical potentials becomes the driving force for dissolution (in the case of undersaturation) or precipitation (in the case of supersaturation). Once nuclei form in a supersaturated solution, they begin to grow by accretion and, as a result, the concentration of the remaining materials drops. Thus, there is a competition for material between the processes of nucleation and crystal growth. The more rapid the nucleation, the larger the number of nuclei formed before relief of supersaturation occurs, resulting in final crystal with smaller size. Brown and LaCroix [26] determined that the nucleation in ettringite formation was diffusion controlled. It has also been suggested that the  $C_3A$  surface may serve as a vehicle for ettringite nucleation [27]. Silva and

Monteiro [16] also observed the ettringite growth on or near the  $C_3A$  surface. On the other hand, Minard et al. [23] assumed that while the slow process of ettringite formation could be limited by ettringite growth rate, its dependence on the surface area of  $C_3A$  indicated that it is limited by dissolution of  $C_3A$ .

Minard et al [23] described that even with different  $C_3A$  reactivity, the time necessary to exhaust the totality of the sulfate ions does not evolve in a linear way with the quantity of gypsum initially introduced. In the present research, the hydration of cubic  $C_3A$  (pure) seems to be more susceptible to the presence of higher concentration of sulfate ions – considering less  $C_3A$  particles in solution for the same initial sulfate concentration. The crystal growth of the hydration products from the cubic sample was more rapid with a larger number of nuclei, which leads to a smaller crystal size, depending on the concentration of sulfate ions. The higher the sulfate concentration, the smaller the size of ettringite needles, the faster the consum of the entire particle of  $C_3A$ . All orthorhombic  $C_3A$  (Na-doped) samples were characterized by the growth of bigger ettringite needles, with the apperance of an intermediate gel stage before the formation of long ettringite needles. For the orthorhombic samples, the higher the sulfate concetration, the smaler are the ettringite size, the longer are the time to exhaust the reaction. Corroborating, but in diferent mixture proportions, Kirchheim et al [11] showed that, in a SEM study, the ettringite crystals, when based on the size and the consumption of  $C_3A$  and gypsum, orthorhombic  $C_3A$  pastes presented a faster rate of formation of crystals, which were also longer. Real time Rheometric measurements showed that orthorhombic  $C_3A$  mixes presented higher increase of stiffness than cubic  $C_3A$  at very early stages of hydration which can be adressed to a higher reactivity of the orthorhombic  $C_3A$  in presence of sulfates.

## 5. Conclusion

Analyzing the hydration of cubic and orthorhombic  $C_3A$  under certain conditions can be summarized as follows:

- The higher the initial solution/aluminate ratio ( $s/a_{\text{initial}} = 50$  ml/g), the greater the sulfate amount available in the reaction, the lower the number of particles of  $C_3A$  in solution, which increased the sulfates/aluminates ratio. This allowed for observation of the complete dissolution of  $C_3A$  particles and precipitation of ettringite crystals.
- For the  $s/a_{\text{initial}} = 10$  ml/g solution, the formation of needles was observed near the surface of particles of cubic  $C_3A$  and a gel appeared between the particles of orthorhombic  $C_3A$ , which was followed by the formation of ettringite needles on this gel.
- For the  $s/a_{\text{initial}} = 5$  ml/g solution, the products of hydration formed almost instantaneously, for both forms of  $C_3A$ . The cubic  $C_3A$  had grew, instantaneously, aciculares crystals. For the orthorhombic  $C_3A$  samples, a gel and hexagonal platelets appeared close to the particles. All reactions had occurred before 50 minutes of hydration.

Soft X-ray microscopy has been shown to be an interesting *in-situ* technique to study real-time hydration of cement phases, particularly cubic and orthorhombic  $C_3A$  providing valuable information about the morphology and growth rate of the hydration products.

## Acknowledgments

The authors acknowledge the financial support of PNPd-CAPES (Programa Nacional de Pós-doutorado da Fundação Coordenação de Aperfeiçoamento de Pessoal de Nível Superior – Ministério da Educação – Brasil) and are grateful to Dong-Hyun Kim and Anne Sakdinawat (Center for X-ray Optics) for their assistance in acquiring the X-ray images. The operation of the microscope is supported by the Director, Office of Science, Office of Basic Energy Sciences, Materials Sciences and Engineering Division, of the U.S. Department of Energy under Contract No. DE-AC02-05-CH11231. Paulo Monteiro acknowledges the financial support given by KAUST.

## References

1. Goetz-Neunhoeffler F, Neubauer J. Crystal structure refinement of Na-substituted  $C_3A$  by Rietveld analysis and quantification in OPC. Proceedings 10<sup>th</sup> Int Congr Chem Of Cem, Göteborg, Sweden, vol 1, 1997.
2. Spierings GACM, Stein HN. The influence of  $Na_2O$  on the hydration of  $C_3A$ . I. Paste hydration. Cem Concr Res, 1976. 6(2): p. 265-272.
3. Wachtler H-J, et al. Über den Einfluss Brennstoffbedingter Akzessorien auf die Hydratation des Trikalziumaluminats. Silikattechnik, 1986. 4: p. 127-131
4. Taylor FW. Cement Chemistry. 1990, London: Academic Press
5. Maki I. Nature of the prismatic dark interstitial material in Portland cement clinker. Cem Concr Res, 1973. 3(3): p. 295-313.
6. Takeuchi Y, Nishi F *et al.* Structural aspect of the  $C_3A$ - $Na_2O$  solid solutions. Proceedings 7<sup>th</sup> Int Congr Chem of Cem. Paris, 1980. 426-431 p.
7. Gobbo L, Sant'agostino L, *et al.*  $C_3A$  polymorphs related to industrial clinker alkalies content. Cem Concr Res, v.34, n.4, p.657-664. 2004.
8. Massazza F, Daimon M. Chemistry of Hydration of Cements and Cementitious systems. Proceedings 9th Int Congr Chem of Cem. New Dehli, India, 1992.
9. Mehta PK, Monteiro PJM. Concrete - Microstructure, Properties and Materials. Third Edition, 2006, New York: McGraw-Hill.
10. Kirchheim AP. Cubic and orthorhombic tricalcium aluminate: analysis of in situ hydration and products. PhD Thesis (in portuguese), Porto Alegre, Brazil, Federal University of Rio Grande do Sul, 2008.
11. Kirchheim AP, et al. Analysis of cubic and orthorhombic  $C_3A$  hydration in presence of gypsum and lime. J Mat Sci, 2009(44): p. 2038-2045.
12. Regourd M, Chromy S, Hjoth L, Mortureux B, Guinier A. Polymorphisme des solutions solides du sodium dans l'aluminate tricalcique. J Appl Cryst (1973). 6, p. 355-364
13. Meyer-Ilse W, et al. X-ray microscopy in Berkeley, in X-ray Microscopy and Spectromicroscopy, J. Thieme et al. (eds) Springer Berlin, (1998) I-1
14. Chao W, et al. Soft x-ray microscopy at a spatial resolution better than 15 nm. Nature, v.435, p.1210-1213. 2005.
15. Kim D-H, Fischer P, Chao W, Anderson E, Im M-Y, Shin S-C, Choe S-B. Magnetic soft X-ray microscopy at 15nm resolution probing nanoscale local magnetic hysteresis (invited), J Appl Phys 99, 08H303 (2006) also selected in Virtual Journal of Nanoscale Science & Technology, 13(17) May 1, 2006
16. Silva DA, Monteiro PJM. Early Formation of Ettringite in Tricalcium Aluminate–Calcium Hydroxide–Gypsum Dispersions. J Am Ceram Soc, 2007. 90: p. 614-617
17. Monteiro PJM, et al. Characterizing the nano and micro structure of concrete to improve its durability. Cem Concr Comp, 2009(in press).
18. Meredith P, et al. Tricalcium aluminate hydration: Microstructural observations by in-situ electron microscopy. J Mat Sci 2004. 39 p. 997- 1005.
19. Scrivener K L, Pratt PL. Microstructural studies of the hydration of  $C_3A$  and  $C_4AF$  independently and in cement paste. Brit Ceram Proc 35 (1984) 207-219.
20. Glasser FP, Marinho MB. Early stages of the hydration of tricalcium aluminate and its sodium-containing solid solutions. Brit Cer Soc, 1984. 35.
21. Locher FW. Cement: Principles of Production and Use. 2006: Vbt Verlag Bau U. Technik
22. Stein HN. The colloid chemistry of calcium aluminate hydrates. Proceedings 7<sup>th</sup> Int Cong Chem of Cem. Paris, 1980. 449-454 p.
23. Minard H, et al. Mechanisms and parameters controlling the tricalcium aluminate reactivity in the presence of gypsum. Cem Concr Res, 2007. 37(10): p. 1418-1426.
24. Billingham J, Coveney PV. Simple Chemical Clock Reactions: Application to Cement Hydration. J Chem Soc Faraday Trans, 1993. 89(16): p. 3021-3028.
25. Mullin JW. Crystallization. London: Butterworths. 1961

26. Brown PW, LaCroix P. The kinetics of ettringite formation. *Cem Concr Res*, 1989. 19: p. 879-884.
27. Pommersheim J, Chang J. Kinetics of hydration of tricalcium aluminate in the presence of gypsum. *Cem Concr Res*, 1988. 18(6): p. 911-922.

### **DISCLAIMER**

This document was prepared as an account of work sponsored by the United States Government. While this document is believed to contain correct information, neither the United States Government nor any agency thereof, nor The Regents of the University of California, nor any of their employees, makes any warranty, express or implied, or assumes any legal responsibility for the accuracy, completeness, or usefulness of any information, apparatus, product, or process disclosed, or represents that its use would not infringe privately owned rights. Reference herein to any specific commercial product, process, or service by its trade name, trademark, manufacturer, or otherwise, does not necessarily constitute or imply its endorsement, recommendation, or favoring by the United States Government or any agency thereof, or The Regents of the University of California. The views and opinions of authors expressed herein do not necessarily state or reflect those of the United States Government or any agency thereof or The Regents of the University of California.